Available online at www.sciencedirect.com
SCIENCE DIRECT®
Journal of Solid State Chemistry 177 (2004) 4494–4500
JOURNAL OF SOLID STATE CHEMISTRY
www.elsevier.com/locate/jssc

Role of doping and CuO segregation in improving the giant permittivity of $CaCu_3Ti_4O_{12}$

D. Capsoni[a,b], M. Bini[a], V. Massarotti[a,b,*], G. Chiodelli[b], M.C. Mozzatic[a], C.B. Azzoni[c]

[a] *Dipartimento di Chimica Fisica "M. Rolla" dell'Università, Università degli Studi di Pavia, viale Taramelli 16, IT 27100 Pavia, Italy*
[b] *CNR-IENI, Sezione di Pavia, viale Taramelli 16, 27100 Pavia, Italy*
[c] *INFM-Dipartimento di Fisica "A. Volta" dell'Università, via Bassi 6, 27100 Pavia, Italy*

Received 23 July 2004; received in revised form 9 September 2004; accepted 10 September 2004
Available online 11 November 2004

Abstract

The dopant role on the electric and dielectric properties of the perovskite-type $CaCu_3Ti_4O_{12}$ (CCTO) compound is evidenced. Impedance spectroscopy measurements show that the relevant permittivity value attributed to sintered CCTO is due to grain boundary (g.b.) effects. The g.b. permittivity value of the pure CCTO can be increased of 1–2 orders of magnitude by cation substitution on Ti site and/or segregation of CuO phase, while the bulk permittivity keeps values $90 < \varepsilon_r < 180$. Bulk and g.b. conductivity contributions are discussed: electrons are responsible for the charge transport and a mean bulk activation energy of 0.07 eV is obtained at room temperature for all the examined samples. The g.b. activation energy ranges between 0.54 and 0.76 eV. Defect models related to the transport properties are proposed, supported by electron paramagnetic resonance measurements.

Keywords: $CaCu_3Ti_4O_{12}$; Cation doping; EPR; Defect models; Impedance spectroscopy; Conductivity measurements; Grain boundary; Giant permittivity; Diffraction profile refinement

1. Introduction

The $CaCu_3Ti_4O_{12}$ (CCTO) perovskite-type compound, with a structure based on body centered cubic cell [1,2], exhibits the so-called "giant-dielectric permittivity phenomenon" [3]. Many works reported about electrical and optical measurements on single crystals [4,5], thin films [6,7] and powders [8–10] evidencing the very high relative permittivity ($\sim 10^4$) and describing the transport properties ($\rho \sim 10^7\,\Omega$ cm at room temperature (RT)). Recent papers investigated about the intrinsic or extrinsic origin of this "giant permittivity" both by theoretical calculations [11] and experiments [9] assessing the role of twinning, for the CCTO single crystals [4,5], and of grain boundary (g.b.), for the powders, both giving rise to the so-called internal barrier layer capacitance (IBLC) effect.

For what concerns the impurity effect on the dielectric properties of CCTO, recent results showed that a 2% substitution of Mn on Cu site quenches the permittivity value to about 100 in the temperature range 300–4.2 K [12]. We recently studied the electron paramagnetic resonance (EPR) [2] and Raman [13] responses of pure and 2%-doped CCTO samples. We also discussed [14], together with the dielectric and transport properties of the pure CCTO, an unexpected enhancement of the permittivity value in a Co 5%-doped sample.

In this work we extend our studies on CCTO samples with substitutions up to 5% of Ca and/or Ti ions, by using X-ray powder diffraction (XRPD), impedance spectroscopy (IS) and EPR measurements. Substitutional and vacancy defect models are also proposed to throw light on the transport properties, taking into account the EPR response of the samples.

*Corresponding author. Dipartimento di Chimica Fisica "M. Rolla" dell'Università, Università degli Studi di Pavia, viale Taramelli 16, IT 27100 Pavia, Italy. Fax: +39 0382 507575.
E-mail address: vincenzo.massarotti@unipv.it (V. Massarotti).

0022-4596/$ - see front matter © 2004 Elsevier Inc. All rights reserved.
doi:10.1016/j.jssc.2004.09.009

2. Experimental

A CCTO pure sample was prepared via solid-state synthesis from a mixture of $CaCO_3$, TiO_2 and CuO ground in an agata mortar. In the following this sample will be reported as pure-ns. A series of pure and substituted CCTO samples was prepared from mechanically ground (30 min) mixtures of the same carbonate and oxides adding the proper amounts of doping components to obtain 2% and/or 5% of cation substitution on Ca or Ti sites leading to the chemical formulas $Ca_{1-x}A_xCu_3Ti_4O_{12}$ and $CaCu_3Ti_{4-y}B_yO_{12}$ (A = La, Sr and $x = 0.02$, 0.05; B = V, Cr, Mn, Ni, Fe, Co and $y = 0.08$, 0.20). Four thermal treatments at 1273 K for 21 h, with intermediate grinding, were performed on each mixture, then the powders were pelletized and treated 16 h at 1323 K for the electrical characterization.

XRPD measurements were performed with a Bruker D5005 diffractometer provided with a curved graphite monochromator on the diffracted beam. Cu$K\alpha$ radiation was used. The Rietveld method [15] was employed to refine the structural and profile parameters and quantify the impurity phases in the final product.

IS measurements were performed on the disk-shaped samples, in the frequency range 10^{-3}–10^{7} Hz with the experimental setting described elsewhere [14], leaving out the Cr 5%-doped sample not obtainable in pellet. The two electrodes were obtained by platinum sputtering the opposite surfaces of the pellets.

EPR measurements were carried out at about 9.4 GHz [2]. Particular care was paid in determining the sample mass and position in the resonant cavity to compare signal intensities (areas): different measurements on the same samples with linewidth $\Delta B < 10$ mT showed intensity variation of a few percent.

3. Results

3.1. X-ray diffraction measurements

All the samples show the diffraction lines pertinent to the CCTO cubic structure [1]. In some cases other lines are observed due to impurity phases, such as CuO and $CaTiO_3$: their amounts are reported in Table 1. In the same table it can be observed that pure-ns sample contains a very slight amount of CuO phase, possibly due to the minor grinding efficiency. The lattice parameters and the bond length were obtained from structural refinement by the Rietveld method: the a value generally increases with dopant percentage. The highest a value, pertinent to Co 5%-doped sample, leads to an increase of 0.08% with respect to the pure CCTO value. Also, the Cu–O, Ca–O and Ti–O bond lengths show only very small variations with doping.

Table 1
Impurity wt% amount determined by Rietveld method

Dopant (%)		CuO (%)	$CaTiO_3$ (%)
Pure		—	—
Pure-ns		0.5	—
La	2	—	—
	5	—	—
Sr	5	—	—
V	2	—	—
Cr	2	—	—
	5	1.5	—
Mn	2	—	—
	5	—	—
Fe	2	0.6	—
	5	2.3	—
Co	2	1.5	—
	5	4.6	0.7
Ni	2	1.7	0.6
	5	6.3	2.2

3.2. Impedance spectroscopy

By plotting the imaginary vs. real part of the complex impedance Z, the contribution of the bulk and g.b. to the resistivity and to the specific capacitance can be estimated. At RT the samples can be classified into four classes and the Fig. 1 shows the related IS plots:

(a) A unique half-circle is observed (see, e.g., the Z'' vs. Z' graph of the La 2% sample in Fig. 1a), even if the intercept does not coincide with the origin (see inset), as previously described for pure [9,14] and some doped CCTO samples [14].
(b) The bulk contribution to the impedance is observable but the g.b. effect is predominant (see, e.g., the graph of the V 2%-doped sample in Fig. 1b).
(c) A comparable bulk and g.b. effect is observed (see, e.g., the graph of the Cr 2%-doped sample in Fig. 1c).
(d) The bulk contribution is predominant and a small contribution of the g.b. to the impedance is observed (see, e.g., the graph of the Mn 2%-doped sample in Fig. 1d).

Resistivity, specific capacitance and dielectric permittivity values at RT due to bulk and g.b. contributions of all the samples are reported in Table 2. For the (a) samples, the bulk capacitance was evaluated with low temperature measurements, as previously shown for pure CCTO [14]. For the (d) samples the g.b. capacitance cannot be obtained because the bulk contribution covers the whole frequency range, so the deconvolution of small right half-circle cannot be performed. For La 5%-doped sample, pertaining to case (d), only overall resistivity and capacitance values ($3.8 \times 10^8\,\Omega$ cm and 50 pF cm^{-1}) can be obtained.

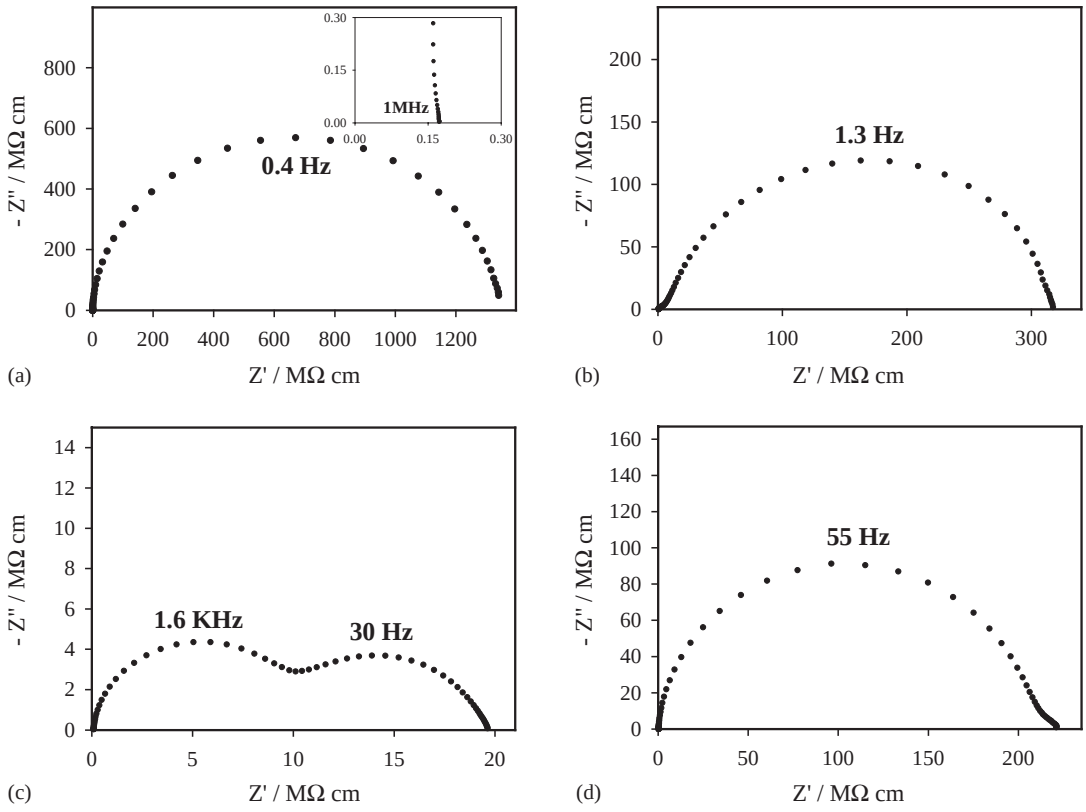

Fig. 1. Impedance plots of: (a) La2%, (b) V 2%, (c) Cr 2% and (d) Mn2%-doped samples. The inset in Fig. 1a shows, in the same units, an enlarged view of the high-frequency region.

Table 2
Specific resistivity, capacitance and permittivity values for both bulk and grain boundary contribution determined by IS

Sample	Bulk			Grain boundary		
	ρ (Ω cm)	C (pF cm^{-1})	ε_r	ρ (Ω cm)	C_{gb} (pF cm^{-1})	$\varepsilon_{r,exp}$
Case a						
Pure	320	12	136	1.7×10^9	300	3400
Pure-ns	75	16	180	6.8×10^7	8700	98,000
La 2%	267	16	180	1.3×10^9	300	3400
Sr 5%	158	14	158	1.3×10^8	2300	26,000
Co 2%	88	12	136	1.4×10^7	5200	59,000
Co 5%	112	13	147	3.1×10^6	13,000	147,000
Ni 2%	75	15	170	1.0×10^7	8800	99,000
Ni 5%	207	11	124	1.1×10^6	10,000	113,000
Case b						
Fe 2%	2.2×10^7	12	136	6.6×10^8	6000	68,000
V 2%	5.3×10^6	8	90	3.1×10^8	400	4500
Case c						
Cr 2%	1.1×10^7	9	102	1.0×10^7	500	5600
Fe 5%	1.5×10^7	10	113	1.3×10^7	4000	45,000
Case d						
Mn 2%	2.1×10^8	14	158	$\sim 1 \times 10^7$	—	—
Mn 5%	1.4×10^8	9	102	$\sim 4 \times 10^6$	—	—

3.3. Conductivity and thermoelectric power

Arrhenius plots related to the bulk conductivity of pure, pure-ns, and some doped samples are shown in Fig. 2a. Two T ranges of linear trend can be observed and the activation energies (E_a), corresponding to the two different slopes, are reported in Table 3 for all the samples, but for those whose g.b. large frequency domain inhibits the estimation of the bulk resistivity. In the 15–40 K range the mean E_a value is about 0.003 eV. At high temperature (100–300 K) the values range between 0.059 and 0.091 eV.

Fig. 2b shows Arrhenius plots pertinent to the g.b. conductivity. The relative E_a values, ranging between 0.54 and 0.76 eV, are reported in the last column of Table 3.

The measured negative Seebek coefficients α, ranging from -99 to $-60\,\mu V/K$ for $473 < T < 673$ K, indicate the electronic nature of the charge carriers in these compounds.

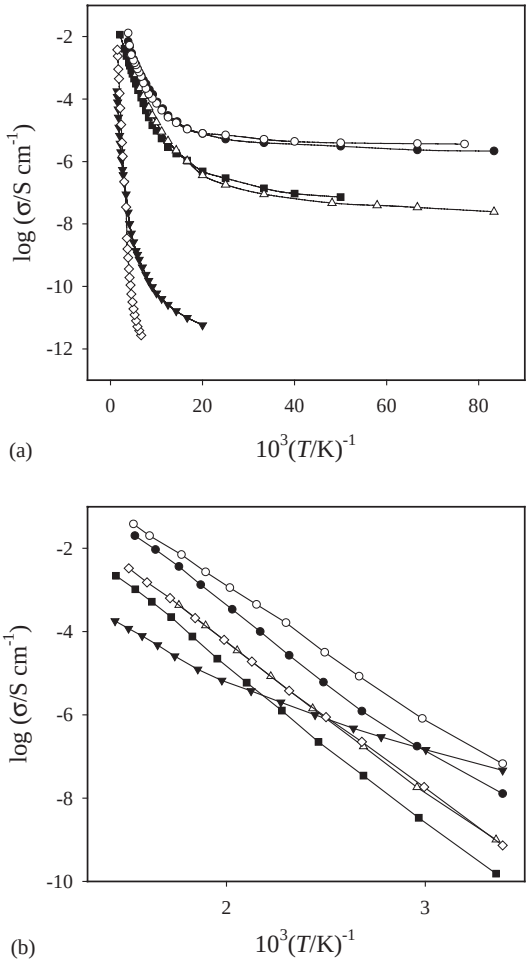

Fig. 2. The Arrhenius plot of La2% (△), Fe2% (◇), Co2% (○), Cr2% (▼) compared with that of the pure (■) and pure-ns (●) ones for the (a) bulk and for (b) grain boundary conductivity contributions.

Table 3
Activation energy for bulk and grain boundary conducting process in the indicated temperature ranges

	Bulk E_a (eV)		g.b. E_a (eV) $T = 323$–673 K
	$T = 15$–40 K	$T = 100$–300 K	
Pure	0.005(1)	0.076(2)	0.76(2)
Pure-ns	0.002(1)	0.059(3)	0.73(3)
Co 2%	0.002(1)	0.068(3)	0.64(2)
La 2%	0.003(1)	0.074(3)	0.71(3)
Cr 2%	—	0.079(3)	0.54(2)[b]
Fe 2%	—	0.091(7)[a]	0.70(3)
V 2%	—	—	0.67(3)
Co 5%	—	—	0.58(3)
Sr 5%	—	—	0.70(3)

[a] T range: 150–190 K.
[b] T range: 523–673 K.

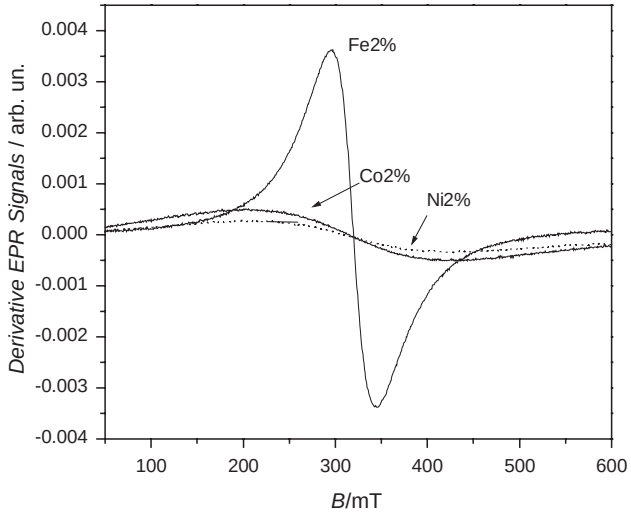

Fig. 3. EPR signals at RT of Fe2%-, Co2%-, Ni2%-doped samples.

3.4. Electron paramagnetic resonance

The EPR spectrum of the pure CCTO sample consists of a structureless symmetric signal centered at $g = 2.15$, with $\Delta B \cong 5.9$ mT at RT and Lorentzian line-shape. Its origin was discussed [2] and attributed to a strong copper-hole ($3d^9$ electronic wave function) delocalization on the four next-neighboring oxygen ions. We also evidenced the effect of 2% substitution of $3d$ ions on Ti site and of La on Ca site. The EPR signals of $3d$ ions substituted samples are well interpreted as superposition of signals with the same g-factor but different ΔB values, or, in some cases, they appear as very broad lines reaching about 230 mT e.g. for Ni- and Co-doped samples, always with the same g-factor (Fig. 3). Similar results are obtained for the 5% substituted CCTO samples on Ti site, as shown in Fig. 4. No evidence of signal components coming from doping ions was found.

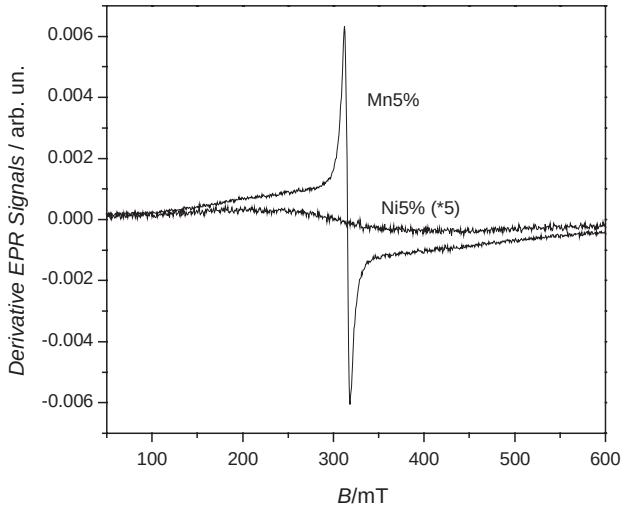

Fig. 4. EPR signals at RT of Mn5%-, Ni5%-doped samples.

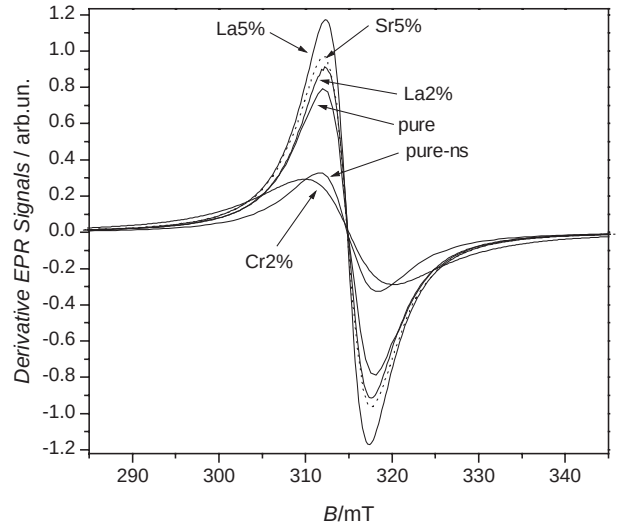

Fig. 5. EPR signals at RT of pure, pure-ns and La5%-, La2%-, Sr5%-, Cr2%-doped samples.

La and Sr substitutions (up to 5%) on Ca site do not modify significantly the signal shape with respect to the pure CCTO signal (Fig. 5). So, for these latter samples and for the pure-ns sample, an easy comparison of the EPR signal intensities is possible. By assuming, at RT, the pure CCTO signal intensity $I_{\text{pure}} = 1$, the following values can be obtained: $I_{\text{La2\%}} = 1.03$, $I_{\text{La5\%}} = 1.05$, $I_{\text{Sr5\%}} = 1$, $I_{\text{pure-ns}} = 0.6$.

The Cr 2%-doped CCTO, without spurious phases, shows a Lorentzian line ($\Delta B = 10$ mT, see Fig. 5) even if with a superimposed very weak broader line with a partial Gaussian shape [13]: for this sample the whole signal EPR intensity, computed by numerical methods, results $I_{\text{Cr2\%}} = 0.89$. For the other transition ions-doped samples a rough intensity evaluation always gives I-values <1.

4. Discussion and conclusions

A series of differently doped samples was considered to evidence the doping influence on the dielectric and transport properties of CCTO. A broad range of specific capacitance, permittivity and resistivity values (from both bulk and g.b. contributions) is obtained at RT, as reported in Table 2. We can observe that cationic substitutions and CuO presence (see Table 1) weakly influence the bulk specific capacitance, being $8 < C < 16\,\text{pF cm}^{-1}$ (or $90 < \varepsilon_r < 180$).

By looking at the g.b. specific capacitance C_{gb}, or the g.b. relative permittivity value $\varepsilon_{\text{r,exp}}$ (Table 2), and at the amount of impurities (Table 1), a connection between the C_{gb} higher values and the CuO presence can be deduced: indeed an increase of C_{gb} with increasing CuO is observed for all the dopant cations but for Fe samples. Observing the results for all the dopant ions in Fig. 6 it is evident that the highest C_{gb} value does not occur at the highest CuO wt% value. The CuO residual phase may increase the C_{gb} values possibly because of its segregation at the boundary, so contributing to an increase of disorder in that region. The comparison of the pure and pure-ns samples, puts into evidence the role played by CuO spurious phase: the two samples, highly different in $\varepsilon_{\text{r,exp}}$ value (3400 and 98,000, respectively), differ only for the presence of CuO phase but pertain to the same class (see Table 2) for what concerns the microstructure. Anyway, some effect is also played by the dopant on the increase of the C_{gb} values. On the other hand, a previous work [8] showed that the only Cu deficiency causes a significant lowering of permittivity value with decreasing the Cu content in CCTO. For our samples where CuO phase is not observed (Table 1), the C_{gb} value is lower, even though maintaining high values (Table 2). About the type of dopant we observe that the La 2%, V 2%

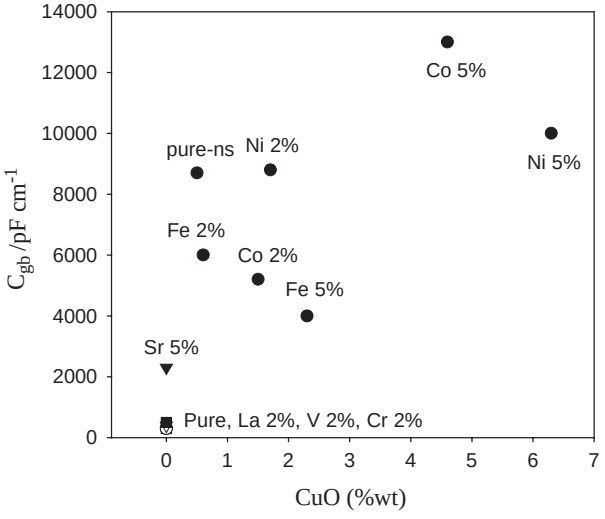

Fig. 6. Grain boundary capacitance as a function of CuO spurious phase percentage.

and Cr 2% substitutions do not influence significantly C_{gb} with respect to the pure CCTO. Other substitutions show significant changes, in particular the greatest effect is obtained by substituting Fe, Co and Ni (Table 2) although CuO impurity is present. Indeed, some kind of cationic substitution in CCTO can deeply modify the grain surface so creating high efficiency (capacitive) dielectric layers: doped (a) samples can reach $\varepsilon_{r,exp}$ values as great as 50 times the pure CCTO value ($\varepsilon_{r,exp} \sim 150,000$ for Co 5%-doped sample). Besides we observed that the lattice parameters depend both on doping ion and its amount, while the bond length shows only minor variation. This also suggests that g.b. effects are responsible for the giant dielectric permittivity. For these compounds, very peculiar g.b. dielectric properties are obtained following a one-step synthesis process, differently from traditional ceramic materials [16].

Concerning the transport properties, a relatively high bulk conduction combined with a highly resistive g.b. was previously reported for CCTO powders [9,14] and thin films [7]. For our (a) samples, the g.b. resistivity contribution ranges from 10^6 to $10^9\,\Omega$ cm and the bulk resistivity contribution from 75 to 320 Ω cm (Table 2). For the other samples, comparable bulk and g.b. contributions are found. Anyway, the negative values of the Seebek coefficient α confirm that the charge carriers are electrons: this result agrees with the more conductive behavior of the pure CCTO observed in N_2 flow with respect to the result obtained in O_2 flow.

We suggest now some defect models to try to explain the complex conductivity behavior. They must be related with EPR results, because the observed signal intensity variations can be attributed to $Cu^{2+} \leftrightarrow Cu^{3+}$ valence changes, if we remember that Cu^{3+} in square planar coordination does not exhibit any EPR signal [17]. Besides, no signal is expected from Cu^{2+} in CuO phase [18], so that only the Cu^{2+} ions in the square planar coordination of the CCTO phase are responsible of the EPR signal, even when the CuO phase is present.

The $CaCu_3Ti_4O_{12}$ compound can be seen as a semiconductor: delocalized electrons in CuO_4 square planar polyhedra (first coordination), possibly in connection with 2nd and 3rd square coordination (conduction band CB), are balanced by holes [2] (Cu^{3+}) in the valence band VB. Therefore,

$$Cu_{Cu}^{2+} \leftrightarrows Cu_{Cu}^{3+} + e^-. \quad (1)$$

If x represents the Cu^{3+} amount, the resulting formula is $CaCu_{3-x}^{2+}Cu_x^{3+}Ti_4O_{12}$ with the corresponding xe^- in the CB.

By neglecting oxygen vacancies, being all the samples sintered in air, and without the CuO spurious phase, a cation M^{z+} (with $z<4$), substituted on the Ti site in a y amount, would give rise to holes in the VB following the equilibrium:

$$\text{Zero} \leftrightarrows M_{Ti}^{(4-z)-} + (4-z)\text{p} \quad (2)$$

The increase in p (Cu^{3+}) implies an EPR signal intensity lowering, as indeed observed for the Cr- and Mn-doped samples ($I_{Cr2\%}$, $I_{Mn2\%} < 1$). If the p-increase also corresponds to an n-decrease, according to the equilibrium (1), by supposing an intrinsic behavior at high temperature, a conductivity lowering is also expected.

Let us consider now the only Cu vacancies effect due to the presence of the spurious CuO phase (Table 1) as for the pure-ns CCTO. The following defect equilibrium can be considered:

$$\text{Zero} \leftrightarrows V_{Cu}^{2-} + 2(Cu_{Cu}^{3+})^+. \quad (3)$$

The Cu^{2+} decrease due both to Cu understoichiometry and Cu^{3+} formation according to (3), should induce a decrease of the EPR signal three times as much the vacancy percentage, each Cu^{2+} vacancy producing two $Cu^{2+} \rightarrow Cu^{3+}$ oxidation processes. Indeed, the pure-ns sample signal area is reduced to 60% with respect to the pure CCTO.

In the Co-, Ni- and Fe-doped samples where the CuO phase is present, both (2) and (3) equilibria should be considered, again leading to a decrease of the EPR signal, as indeed observed, even if it is difficult to quantify the related effects on the EPR signal area, due to high ΔB values (Figs. 3, 4).

For substitutions on Ca site, no variation is expected with bivalent cations, such as Sr, and no changes in the EPR signal area are indeed observed. Otherwise the La^{3+} substitution would lead to

$$\text{Zero} \leftrightarrows La_{Ca}^{+} + 1e^-(\text{BC}) \quad (4)$$

displacing equilibrium (1) towards Cu^{2+}, leading to an EPR signal increase ($I_{La2\%} = 1.03$, $I_{La5\%} = 1.05$).

Being the bulk conductivity due to electron transport, the equilibria involving electrons increase or decrease should influence the samples conductivity. From Table 2 very low bulk conductivity results for the transition ions-doped samples, in agreement with the equilibria (2) and (1), but for Co- and Ni-doped samples, containing CuO. The pure-ns, also containing CuO, is more conducting than the pure CCTO sample, in spite of the proposed models. For what concerns the Fe 2% sample, with a very low CuO content, the low conductivity can be related to a possibly bivalent stable oxidation state (high influence of equilibrium (2)). Anyway the bulk conductivity behavior of samples containing some amounts of CuO phase (Fig. 6) cannot be easily explained.

Concerning the substitutions in the Ca site, the La 2%-doped sample is a little bit more conductive than stoichiometric CCTO (Fig. 2a and Table 2), in agreement with the proposed equilibria (4) and (1).

Nevertheless, an unexpected bulk conductivity increase is observed for the Sr-doped sample (Table 2).

About the g.b. resistivity contribution the spread of the values ranging from 10^6 to $10^9\,\Omega$cm at RT, irrespective of the samples classes, prevents any correlation with the dopant type and amount and with the presence of spurious phases.

The bulk and g.b. conduction mechanisms are thermally activated. For the bulk, the slope in the Arrhenius plot shows two linear regions (100–300 K and 15–40 K, see Fig. 2) for which two different activation energies (E_a) can be estimated (Table 3). In the 100–300 K range the E_a value of about 0.07 eV, very similar for all the samples, is a typical value of electron hopping energy in agreement with that obtained by Sinclair et al. [9]. The gradual slope variation below 100 K and the very low E_a values (0.001–0.005 eV) between 15 and 40 K, already observed and discussed for the pure sample, can be attributed to the Anderson localization [19]. For what concerns the g.b., E_a values ranging between 0.54 and 0.76 eV in the 323–673 K temperature region have been obtained. These E_a values, significantly higher than those observed for the bulk conductivity, indicate a possible barrier activation energy contribution due to disorder and heterogeneity typical of the grain boundary.

In conclusions, this work puts into evidence the dopants role and the CuO spurious phase segregation effect on the transport and dielectric properties of doped CCTO samples.

The IS measurements allowed us to separate the transport contributions of the bulk and grain boundary: the former, with an electron hopping semiconducting behavior, and the latter more insulating. The proposed defect models, supported by EPR measurements, can explain the bulk conductivity behavior at least for samples without CuO phase.

About the dielectric properties, the relevant grain boundary permittivity value of the pure sample ($\varepsilon_{r,exp} = 3400$) can be significantly increased by both doping with Fe, Co and Ni on Ti site and by CuO segregation. Instead, the bulk permittivity is lightly influenced by doping ($90 < \varepsilon_r < 180$, typical of many perovskitic compounds), so suggesting that only g.b. effects are responsible for the observed giant dielectric permittivity.

This work evidences that, through a simple solid state reaction at moderate temperature (1323 K) in air, an internal barrier layer capacitance (IBLC) material is obtained: with a suitable choice of dopant, the dielectric performance of the pure material can be improved making the doped CCTO more interesting for applications in the electronic industry.

Acknowledgments

This work was partially supported by "Consorzio per i Sistemi a Grande Interfase" (CSGI) and IENI-CNR, Department of Pavia.

References

[1] B. Bochu, M.N. Deschizeauix, J.C. Joubert, A. Collomb, J. Chenavas, M. Marezio, J. Solid State Chem. 29 (1979) 291–298.
[2] M.C. Mozzati, C.B. Azzoni, D. Capsoni, M. Bini, V. Massarotti, J. Phys.: Condens. Matter 15 (2003) 7365–7374.
[3] A.P. Ramirez, M.A. Subramanian, M. Gardel, G. Blumberg, D. Li, T. Vogt, S.M. Shapiro, Solid State Commun. 115 (2000) 217–220.
[4] C.C. Homes, T. Vogt, S.M. Shapiro, S. Wakimoto, A.P. Ramirez, Science 293 (2001) 673–676.
[5] C.C. Homes, T. Vogt, S.M. Shapiro, S. Wakimoto, A.P. Ramirez, Phys. Rev. B 67 (2003) 092106/1-4.
[6] W. Si, E.M. Cruz, P.D. Johnson, P.W. Barnes, P. Woodward, A.P. Ramirez, Appl. Phys. Lett. 81 (2002) 2056–2058.
[7] A. Tselev, C.M. Brooks, S.M. Anlage, H. Zeng, L. Salamanca-Riba, R. Ramesh, M.A. Subramanian, Phys. Rev. B 70 (2004) 144101/1–8.
[8] M.A. Subramanian, D. Li, N. Duan, B.A. Reisner, A.W. Sleight, J. Solid State Chem. 151 (2000) 323–325.
[9] D.C. Sinclair, T.B. Adams, F.D. Morrison, A.R. West, Appl. Phys. Lett. 80 (2002) 2153–2155.
[10] A.P. Ramirez, G. Lawes, V. Butko, M.A. Subramanian, C.M. Varma, Cond. Matt. (2002) 1–9.
[11] M.H. Cohen, J.B. Neaton, L. He, D. Vanderbilt, J. Appl. Phys. 94 (2003) 3299–3306.
[12] W. Kobayashi, I. Teresaki, Physica B 329–333 (2003) 771–772.
[13] E. Giulotto, M.C. Mozzati, C.B. Azzoni, V. Massarotti, D. Capsoni, M. Bini, Ferroelectrics 298 (2004) 61–67.
[14] G. Chiodelli, V. Massarotti, D. Capsoni, M. Bini, C.B. Azzoni, M.C. Mozzati, P. Lupotto, Solid State Commun. 132 (2004) 241–246.
[15] J. Rodriguez Carvajal, Physica B 192 (1993) 55–69.
[16] G. Chiodelli, A. Magistris, M. Scagliotti, F. Parmigiani, J. Mater. Sci. 23 (1988) 1159–1163.
[17] C.B. Azzoni, A. Paleari, J. Phys.: Condensed Matter 6 (1994) 4699–4705.
[18] C.B. Azzoni, A. Paleari, G.B. Parravicini, J. Phys.: Condensed Matter 4 (1992) 1359–1366.
[19] J. Tateno, Physica C 214 (1993) 377–384.